

A NEW REDSHIFT INDICATOR OF GAMMA-RAY BURSTS TO MEASURE THE COSMOS

Zhibin Zhang*

National Astronomical Observatories/Yunnan Observatory, Chinese Academy of Sciences, Kunming 650011

*Email: zbzhang@ynao.ac.cn

ABSTRACT

Using 64 ms count data of long gamma-ray bursts (LBs, $T_{90} > 2.6$ s), we analyze the quantity named relative spectral lag (RSL), $\tau_{31}/FWHM_{(1)} = \tau_{rel, 31}$. We investigate in detail the properties of the RSL for a sample of nine LBs, using the general cross-correlation technique that includes the lag between two different energy bands. We find that the distribution of RSLs is normal and has a mean value of 0.1. Our important discovery is that redshift (z) and peak luminosity (L_p) are strongly correlated with the RSL, which can be measured easily and directly, making the RSL a good redshift and peak luminosity indicator. In addition, we find that the redshift and luminosity estimator can also hold for short gamma-ray bursts (SBs, $T_{90} < 2.6$ s). With it, we estimate the median of redshift and peak luminosity of SBs to be about $z \leq 0.06$ and $L_p \sim 1.68 \times 10^{48}$ erg/s, which are in excellent agreement with the results suggested by some previous authors. We thus argue that the sources including SBs and LBs with positive spectral lags might be one united category with the same physical process.

Key words: Gamma-rays, Long bursts, Short bursts, Redshift

1 INTRODUCTION

The temporal profiles of gamma-ray bursts (GRBs) generally exhibit very complex and variable characteristics because of overlapping between adjacent pulses (Norris et al. 1996; Quilligan et al., 2002). So far many investigations on the analysis of their light-curves, especially the pulses, have been made. For example, the properties of pulses such as widths, amplitudes, area of pulses, and time intervals between them together with number of pulses per burst has been studied by several authors (e.g. McBreen et al., 1994, 2001, 2003; Hurley et al. 1998; Nakar & Piran, 2002; Qin et al., 2005). In addition, some investigations associated with spectra have also been made (e.g. Kouveliotou et al., 1993; Hurley et al. 1992; Ghirlanda et al., 2004a). In particular, the spectral lag between variation signals in different energy bands not only reflects the features of spectrum evolution but also exhibits the properties of light-curve. Much research regarding this variable has been done from many distinct aspects (see, e.g. Norris et al., 2000, 2001, 2005; Gupta et al., 2002; Kocevski & Liang, 2003; Daigne & Mochkovitch, 2003; Schaefer, 2004; Li et al., 2004; Chen et al., 2005). Interestingly, it is found that unlike SBs the spectral lags of most LBs are larger than zero and concentrate on the short end of the lag distribution near 100 ms (Band, 1997; Norris et al., 2001).

Concerning the redshift (or luminosity) indicators with GRBs, previous investigations have offered us some significant paradigms in the case of light-curves, for instance, the relationship between luminosity-lag (Norris et al., 2000) and luminosity-variability (Reichart et al., 2001). A particular relationship between the lag and the

variability has been strongly confirmed to prove the reliability of both of these luminosity indicators (Schaefer et al., 2001). On the other hand, other indicators based on GRB spectral features are also constructed subsequently. They originate from either the E_p - E_{iso} relation (Amati et al., 2002; Atteia, 2003), the E_p - L_p relation (e.g. Yonetoku et al., 2004), or the E_p - E_γ relation (Ghirlanda et al., 2004b). The spectra and the light-curves are related to each other via the spectral lag.

Norris et al. (2004, 2005) have found that wide pulse width is strongly correlated with spectral lag, and these two parameters may be viewed as mutual surrogates in formulations for estimating GRB luminosity and total energy. Motivated by the above-mentioned developments, our first aim is to analyze the RSLs of LBs in order to see what their distribution is. A further purpose of this work is to search for the possible application of the RSL to cosmological studies.

2 DATA PREPARATION

We use 64 ms count data selected from the current BATSE (Burst And Transient Source Experiment) catalog for LBs, called sample 1, which includes 36 sources. Note that we have only taken into account those bursts with a single pulse in the course of selection. The highly variable temporal structure observed in most bursts is deemed to be produced by internal shocked outflow, provided that the source emitting the relativistic flow is variable enough (e.g. Dermer & Mitman, 1999; Katz, 1994; Rees & Meszaros, 1994; Piran, Shemi, & Narayan, 1993). In this case, the temporal structure generally reflects the activity of the inner engine that drives the bursts (Sari & Piran, 1997). As a result of overlap, it is generally difficult to determine how many pulses complex bursts should comprise or to model the shape of these pulses (Norris et al., 1996; Lee et al., 2000). Fortunately, the observed peaks have almost one-to-one correlation with the activity of the emitting source, that is to say, each pulse is permissively assumed to be associated with a separate emission episode of one burst (Kobayashi et al., 1997; Kocevski et al., 2003). On the other hand, spectra parameters for distinct pulses within a burst are different from each other, which allows us to believe the spectral lags between these pulses will show a large difference (Hakkila & Giblin, 2004; Ryde et al., 2005). Therefore we let our sample be composed of the relatively simple and bright bursts dominated by a single pulse event rather than the dim or multi-peak ones for which we could accurately calculate the spectral lags.

The method of selection is not by an automated program (e.g. Scargle, 1998; Norris et al., 2001; Quilligan et al., 2002) but by directly experienced eyes, which in a certain degree could reduce any biases either from denoising techniques or from the pulse identification algorithm itself (Ryde et al., 2003). Lee et al. (2000) have found the number of the pulses within a burst is usually different between energy bands. In principle, a bright-independent analysis is required as the burst duration measurement needs (Bonnell et al., 1997), whereas the level of S/N should be reasonable and reliable. Based on these considerations, the criteria for our sample selection are now constrained as follows: T90 duration > 2.6 s; BATSE peak flux (50-300 KeV) > 1.5 photons $\text{cm}^{-2}\text{s}^{-1}$; and peak count rate (> 25 KeV) > 14000 counts s^{-1} .

In general, the first step in data preparation is to select the appropriate background for subtraction. To handle these data as a whole, an alternative mode of processing involving background subtraction along with denoising is presented here. For each source, we take the signal data as covering the fullest range of the pulse as possible in order to ensure that the contributions of all signals to lags are considered sufficiently. From the point of view of experience, data beyond this range are regarded as the fit of the background. However, for convenience, we

prefer disposing of all data involving pre- and post-pulse to processing separately.

Considering the duration and background level of LBs, we first smooth them with the DB3 wavelet using MATLAB software and then fit them with a pulse function plus a quadratic form, namely

$$F(t) = F_m \left(\frac{t}{t_m} \right)^r \left[\frac{d}{d+r} + \frac{r}{d+r} \left(\frac{t}{t_m} \right)^{(r+1)} \right]^{-(r+d)/(r+1)} + at^2 + bt + c \quad (1)$$

where the first expression on the right is a quite flexible function (see Eq. (22), Kocevski et al., 2003) applied to describe pulse shapes and the quadratic term represents a background that spans the whole data. The parameter t_m is the time of the maximum flux, F_m , of the pulse, and the quantities r and d are two indexes describing the rise and decay of pulse profiles respectively. Once the background is subtracted from the fitted data, the remainder is pure signal data, called sample 2, and is not contaminated by background and noise beyond a certain error level. These signal data are just what are needed to use for the analysis of spectra and light-curves.

3 RELATIVE SPECTRAL LAG

In this section we focus our attention on measuring RSLs of the single-peaked events from the above signal data for 36 LB pulses. Using sample 2, we cross-correlate energy bands between energy channels j and k with the following cross-correlation function (CCF) (Band, 1997)

$$CCF(\tau; v_j, v_k) = \frac{\langle v_j(t) v_k(t + \tau) \rangle}{\sigma_{v_j} \sigma_{v_k}} \quad (j \neq k) \quad (2)$$

where $\sigma_{v_i} = \langle v_i^2 \rangle^{1/2}$ [$i=1,2,3$, or 4] represents different energy channels; τ is the so-called spectral lag between any two of these channels; and v_j and v_k stand for two time series in which they are the respective light curves in two different energy bands. If the considered channels are $j = 3$ and $k = 1$, the spectral lag can be thus written as τ_{31} , differing from those previous definitions of spectral lag (e.g. Norris et al., 2000; Gupta et al., 2002). We otherwise define a quantity called RSL, namely

$$\tau_{rel, 31} = \tau_{31} / FWHM_{(1)} \quad (3)$$

where τ_{31} represents the lag between energy bands 3 and 1, and $FWHM_{(1)}$ denotes the full width at half maximum of time profile in energy channel 1. The τ_{31} is determined by the location of τ where CCF peaks because the CCF curve on this occasion is smooth and resembles a Gaussian shape near its peak. If the data points close to peak are not dense enough, we interpolate them within the range from one-side of the peak to the other. One could find from this definition that $\tau_{rel, 31}$ is indeed a dimensionless quantity. However, the magnitude of τ_{31} is inevitably influenced by error propagation from the fitted parameters shown in Eq. (1). The detailed error analysis can be found in paper I.

With the above measure, we derive the quantities τ_{31} and $FWHM_{(1)}$ for sample 2 and then calculate $\tau_{rel, 31}$. A plot of the RSLs distribution is illustrated in Figure 1, from which we can find that all the pulses hold positive $\tau_{rel, 31}$ within the range from 0 to 0.35 and they concentrate on an approximate value of 0.1. Moreover, we fit the distribution with a Gaussian function and get $\chi^2/dof = 1.1$ with $R^2 = 0.97$, which indicates that the distribution of RSLs is consistent with a normal distribution. However, the distributions of FWHM and spectral lags (or time

intervals) have been found to follow a log-normal instead of normal form (see e.g. Mcbreen et al., 2003). In the following, we pay particular attention to the physical explanation of $\tau_{rel, 31}$ that makes it a useful tool in astrophysics.

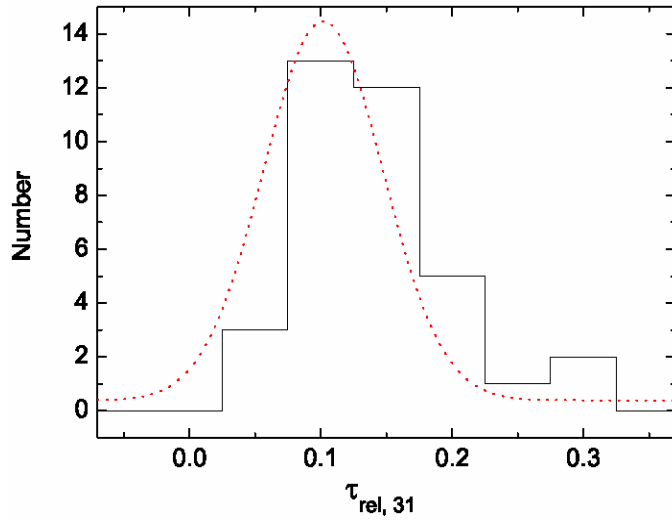


Figure 1. Histogram of the distribution of RSLs for LBs with a sample of 36 bright pulses. The smooth curve is a Gaussian function fitted to the distribution, where the mean value is $\mu=0.102$ and the standard deviation is $\sigma=0.045$.

4 REDSHIFT AND LUMINOSITY INDICATOR

To understand the physical implications of RSLs, we choose one sub-sample, composed of nine long-lag and wide-pulse GRBs with simpler physics owing to more accurate measures, to investigate the relationship of RSL with redshift and luminosity (see Table 1).

Table 1. Parameters for observed and modeled data in sub-sample

Trigger	$\tau_{rel,31}^*$	z^a	$L_p^a(10^{51} erg/s)$
1	2	3	4
1406	0.126 ± 0.017	1.91 ± 0.4	22.8 ± 10
2387	0.127 ± 0.007	3.76 ± 0.4	176 ± 50
2665	0.166 ± 0.014	1.19 ± 0.11	11 ± 2
3257	0.059 ± 0.003	11.97 ± 1.6	1750 ± 600
6504	0.105 ± 0.006	1.67 ± 0.07	40 ± 4
6625	0.101 ± 0.04	2.18 ± 0.4	15.8 ± 6
7293	0.092 ± 0.009	8.48 ± 3	733 ± 500
7588	0.149 ± 0.027	1.44 ± 0.08	7.79 ± 2.2
7648	0.192 ± 0.036	0.43^b	0.54 ± 0.1^c

Notes. Redshift (col. 3) and peak luminosity (col. 4) estimated by the E_p-L_p relation have been borrowed from Yonetoku et al. (2004) due to lack of the information about these sources except for trigger 7648 whose z and L_p ($10^{51} erg/s$) is offered by Galama et al. (1999) and Guidorzi et al. (2005) respectively.

References: a. (Yonetoku et al., 2004); b. (Galama et al., 1999); c. (Guidorzi et al., 2005).

As Atteia (2005) points out, whether redshift indicators are good or not is determined by the degree of correlation

between redshift and the indicators, which are generally combinations of GRB parameters with a small intrinsic scatter. To test the validity of $\tau_{rel,31}$ as the redshift indicator, we contrast the observed data with the theoretical model in Figure 2. From Figure 2 (a) and (b), the best fits to a linear model can be written as

$$\begin{cases} \log z = (1.56 \pm 0.24) - (9.66 \pm 1.86) \tau_{rel,31} \\ \log L_p = (55.44 \pm 0.63) - (23.07 \pm 4.88) \tau_{rel,31} \end{cases} \quad (4)$$

with spearman rank-order correlation coefficients of -0.88 ($P \sim 1.5 \times 10^{-3}$) for the former and -0.83 ($P \sim 5 \times 10^{-3}$) for the latter. This indicates the relatively accurate connection between the RSLs and the redshift (or luminosity) does exist. Provided the $\tau_{rel,31}$ is measured, using Eq. (4) one could precisely estimate redshifts and peak luminosities of those sources without the information of observed spectral lines. From this viewpoint, the quantity $\tau_{rel,31}$ can be regarded as an ideal indicator of redshift and/or luminosity. Meanwhile, the RSLs might be utilized to constrain the cosmological parameters (say, Ω_m , Ω_Λ , H_0) once redshift and luminosity have been determined by Eq. (4) simultaneously. Certainly, the realization of this possibility requires us to eliminate selection effects as much as we can in advance, not only in observations but also in calculations.

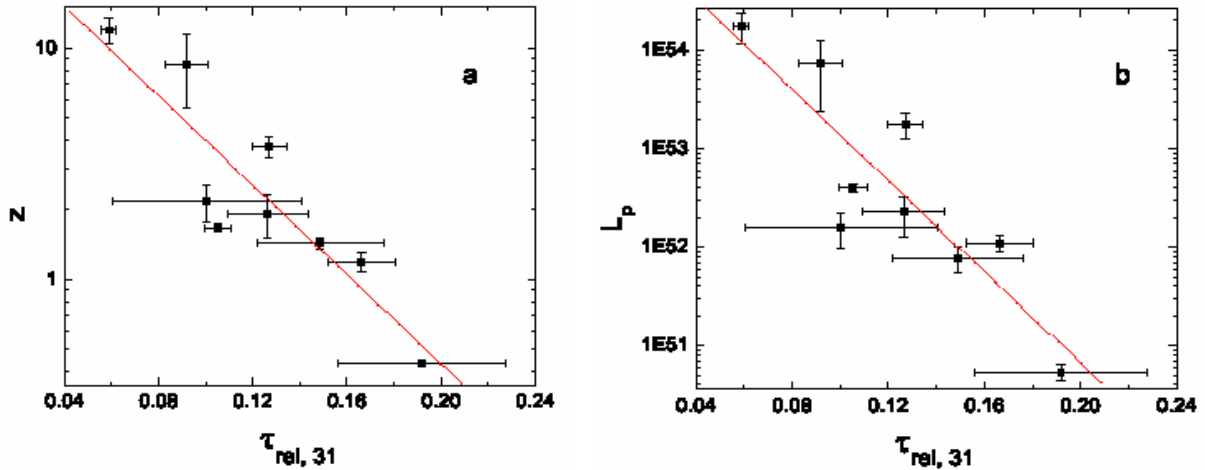


Figure 2. Calibration curves for the relative spectral lags, RSL. Plots of RSL vs. redshift and peak luminosity can be used to calibrate redshift and/or luminosity indicators. The plots here can be fitted to yield Eq. (4) (marked with the straight red lines in panels a and b).

5 APPLICATIONS

As has been known from Eq. (4), the RSL, $\tau_{rel,31}$, could be used as a good redshift and luminosity indicator for LBs. Because pulse widths and spectral lags are respectively proportional to Γ^{-2} approximately (Qin et al., 2004; Zhang & Qin, 2005), RSL could be an intrinsic physical quantity, which allows us to assume that the above two relationships also exist for SBs. In this case we can estimate the redshift and luminosity of SBs with the measured RSLs.

We have found the RSLs of SBs are normally distributed with $\sigma=0.42$ and $\mu=0.082$ (Zhang et al., 2006b). Based on this distribution, we reproduce a sample including 100 sources, from which we select those with positive RSLs as a new sample of 66 SBs. Applying Eq. (4) to this sub-sample we calculate the median redshift to be about 0.03, which is consistent with the result $z \leq 0.06$ (e.g. Ghirlanda et al., 2006) and thus corresponds to

the discovery originated at the low redshift universe for most SBs (Magliocchetti et al., 2003; Tanvir et al., 2005). In addition, we can create from this model a fraction of the SB population at higher redshift $z \leq 6$, which is beyond the range of $z \sim 15-20$ found by Lamb & Reichard (2000; see also Lloyd-Ronning et al., 2002; Schaefer, 2003) but is in agreement with the suggestion of Levan et al. (2006). In that case, the GRBs could be the best candidate to study the very early universe for $z > 6.29$ (e.g. Kawai et al., 2005). Also, we gain the median peak luminosity $\sim 1.68 \times 10^{48}$ erg/s, which is in accordance with the previous estimate (e.g. Guetta & Piran, 2005).

The striking consistency of theories with observations seems to show that both short and long bursts with positive time lags can indeed be united as one category and can have the same redshift and luminosity estimators as Eq. (4). With an increasing number of afterglow observations of SBs, whether or not the redshift and luminosity indicator can also hold for SBs is expected to be answered accurately.

6 ACKNOWLEDGMENTS

I would like to thank Dr D. Kocevski for his helpful discussions on the lags in SBs.

7 REFERENCES

- Amati, L., Frontera, F., Tavani, M., et al. (2002) Intrinsic spectra and energetics of BeppoSAX Gamma-Ray Bursts with known redshifts. *A&A* 390, 81.
- Atteia, J. L. (2003) A simple empirical redshift indicator for gamma-ray bursts. *A&A* 407, L1.
- Atteia, J. L. (2005) Redshift indicators for gamma-ray bursts. *Astro-ph/0505074*.
- Band, D. L. (1997) Gamma-Ray Burst Spectral Evolution through Cross-Correlations of Discriminator Light Curves. *ApJ* 486, 928.
- Bonnell, J. T., Norris, J. P., Nemiroff, R. J., et al. (1997) Brightness-independent Measurements of Gamma-Ray Burst Durations. *ApJ* 490, 79.
- Chen, L., Lou, Y.-Q., Wu, M., et al. (2005) Distribution of Spectral Lags in Gamma-Ray Bursts. *ApJ* 619, 983.
- Daigne, F. & Mochkovitch, R. (2003) The physics of pulses in gamma-ray bursts: emission processes, temporal profiles and time-lags. *MNRAS* 342, 587.
- Dermer, C. D. & Mitman, K. E. (1999) Short-Timescale Variability in the External Shock Model of Gamma-Ray Bursts. *ApJ* 513, L5.
- Ghirlanda, G., Ghisellini, G., & Celotti, A. (2004a) The spectra of short gamma-ray bursts. *A&A* 422, L55.
- Ghirlanda, G., Ghisellini, G., & Lazzati, D. (2004b) The Collimation-corrected Gamma-Ray Burst Energies Correlate with the Peak Energy of Their νF_{ν} Spectrum. *ApJ* 616, 331.

- Ghirlanda, G., et al. (2006) On the correlation of short gamma-ray bursts and clusters of galaxies. *MNRAS* 368, L20.
- Guetta, D. & Piran, T. (2005) The luminosity and redshift distributions of short-duration GRBs. *A & A* 435, 421.
- Gupta, V., Gupta, P. D., & Bhat, P. N. (2002) Study of Spectral Lag for Short GRBs. *astro-ph/0206402*.
- Hakkila, J. & Giblin, T. W. (2004) Quiescent Burst Evidence for Two Distinct Gamma-Ray Burst Emission Components. *ApJ* 610, 361.
- Hurley, K., Kargatis, V., Liang, E., et al. (1992) Spectral variations in gamma-ray bursts. *AIPC* 265, 195.
- Hurley, K. J., McBreen, B., Quilligan, F., et al. (1998) Wavelet Analysis and Lognormal Distributions in GRBS. *AIPC* 428, 191.
- Katz, J. (1994) Two populations and models of gamma-ray bursts. *ApJ* 422, 248.
- Kawai, N., et al. (2005) GRB 050904: Subaru Optical Spectroscopy. *GCN* 3937, 1.
- Kobayashi, S., Piran, T., & Sari, R. (1997) Can Internal Shocks Produce the Variability in Gamma-Ray Bursts? *ApJ* 490, 92.
- Kouveliotou, C., Meegan, C. A., Fishman, G. J., et al. (1993) Identification of two classes of gamma-ray bursts. *ApJ* 413, L101.
- Kocevski, D., Ryde, F., & Liang, E. (2003) Search for Relativistic Curvature Effects in Gamma-Ray Burst Pulses. *ApJ* 596, 389.
- Lamb, D. & Reichart, D. E. (2000) Gamma-Ray Bursts as a Probe of the Very High Redshift Universe. *APJ* 536, 1.
- Levan, A. J., Wynn, G. A., Chapman, R., et al. (2006) Short gamma-ray bursts in old populations: magnetars from white dwarf-white dwarf mergers. *MNRAS* 368, L1.
- Lee, A., Bloom, E. D., & Petrosian, V. (2000) Properties of Gamma-Ray Burst Time Profiles Using Pulse Decomposition Analysis. *ApJS* 131, 1.
- Li, T. P., Qu, J. L., Feng, H., et al. (2004) Timescale Analysis of Spectral Lags. *ChJAA* 4, 583.
- Lloyd-Ronning, N. M., Fryer, C. L., & Ramirez-Ruiz, E. (2002) Cosmological Aspects of Gamma-Ray Bursts: Luminosity Evolution and an Estimate of the Star Formation Rate at High Redshifts. *ApJ* 574, 554.

- Magliocchetti, M., Ghirlanda, G., & Celotti A. (2003) Evidence for anisotropy in the distribution of short-lived gamma-ray bursts. *MNRAS* 343, 255.
- McBreen, B., Hurley, K. J., Long, R., Metcalfe, L. (1994) Lognormal Distributions in Gamma-Ray Bursts and Cosmic Lightning. *MNRAS* 271, 662.
- McBreen, S., Quilligan, F., McBreen, B., et al. (2001) Temporal properties of the short gamma-ray bursts. *A&A* 380, L31.
- McBreen, S., Quilligan, F., McBreen, B., et al. (2003) Temporal Properties of Short and Long Gamma-Ray Bursts. *AIPC* 662, 280.
- Nakar, E. & Piran, T. (2002) Temporal properties of short gamma-ray bursts. *MNRAS* 330, 920.
- Norris, J. P., Nemiroff, R. J., Bonnell, J. T., et al. (1996) Attributes of Pulses in Long Bright Gamma-Ray Bursts. *ApJ* 459, 393.
- Norris, J. P., Marani, G. F., & Bonnell, J. T. (2000) Connection between Energy-dependent Lags and Peak Luminosity in Gamma-Ray Bursts. *ApJ* 534, 248.
- Norris, J. P., Scargle, J. D., & Bonnell, J. T. (2001) Short Gamma-Ray Bursts Are Different. *astro-ph/0105108*.
- Norris, J. P., Bonnell, J. T., Kazanas, D., et al. (2004) Long-Lag, Wide-Pulse, Gamma-Ray Bursts. *AAS* 205, 6804.
- Norris, J. P., Bonnell, J. T., Kazanas D., et al. (2005) Long-Lag, Wide-Pulse Gamma-Ray Bursts. *ApJ* 627, 324.
- Piran, T., Shemi, A., Narayan, R. (1993) Hydrodynamics of Relativistic Fireballs. *MNRAS* 263, 861.
- Qin, Y. P., Zhang, Z. B., Zhang, F. W., et al. (2004) Characteristics of Profiles of Gamma-Ray Burst Pulses Associated with the Doppler Effect of Fireballs. *ApJ* 617, 439.
- Qin, Y. P., Dong, Y. M., Lu, R. J., et al. (2005) Relationship between the Gamma-Ray Burst Pulse Width and Energy Due to the Doppler Effect of Fireballs. *ApJ* 632, 1008.
- Quilligan, F., McBreen, B., Hanlon, L., et al. (2002) Temporal properties of gamma ray bursts as signatures of jets from the central engine. *A &A* 385, 377.
- Rees, M. J., & Meszaros, P. (1994) Unsteady outflow models for cosmological gamma-ray bursts. *ApJ* 430, L93.
- Reichart, D. E., Lamb, D. Q., Fenimore, E. E., et al. (2001) A Possible Cepheid-like Luminosity Estimator for the Long Gamma-Ray Bursts. *ApJ* 552, 57.

- Ryde, F., Borgonovo, L., Larsson, S., et al. (2003) Gamma-ray bursts observed by the INTEGRAL-SPI anticoincidence shield: A study of individual pulses and temporal variability. *A&A* 411, L331.
- Ryde, F., Kocevski, D., Bagoly, Z., et al. (2005) Interpretations of gamma-ray burst spectroscopy. II. Bright BATSE bursts. *A&A* 432, 105.
- Sari, R. & Piran, T. (1997) Variability in Gamma-Ray Bursts: A Clue. *ApJ* 485, 270.
- Scargle, J. D. (1998) Studies in Astronomical Time Series Analysis. V. Bayesian Blocks, a New Method to Analyze Structure in Photon Counting Data. *ApJ* 504, 405.
- Schaefer, B. E., Deng, M., & Band, D. L. (2001) Redshifts and Luminosities for 112 Gamma-Ray Bursts. *ApJ* 563, L123.
- Schaefer, B. E. (2003) Gamma-Ray Burst Hubble Diagram to $z=4.5$. *ApJ* 583, L67.
- Schaefer, B. E. (2004) Explaining the Gamma-Ray Burst Lag/Luminosity Relation. *ApJ* 602, 306.
- Tanvir, N. R., Chapman R., Levan A. J., et al. (2005) An origin in the local Universe for some short gamma-ray bursts. *Nature* 438, 991.
- Yonetoku, D., Murakami, T., Nakamura T., et al. (2004) Gamma-Ray Burst Formation Rate Inferred from the Spectral Peak Energy-Peak Luminosity Relation. *ApJ* 609, 935.
- Zhang, Z. B. & Qin Y. P. (2005) Physical implication of the Kocevski-Ryde-Liang pulse function of gamma-ray bursts. *MNRAS* 363, 1290.
- Zhang, Z. B., et al. (2006a) Relative Spectral Lag: a New Redshift Indicator of Gamma-ray Bursts. *ChJAA* 6, 312 (Paper I).
- Zhang, Z. B., et al. (2006b) Revisiting the characteristics of the spectral lags in short gamma-ray bursts. *MNRAS*, accepted, *astro-ph/0604349*.